Paper

Doping effect of Dy on leakage current and oxygen sensing property of SrTiO₃ thin film prepared by PLD

Naoki WAKIYA,[†] Yusuke KIMURA, Naonori SAKAMOTO, Desheng FU,[*] Toru HARA,[**]
Takashi ISHIGURO,[**] Takanori KIGUCHI,[***] Kazuo SHINOZAKI[****] and Hisao SUZUKI[*]

Department of Materials Science and Chemical Engineering, Shizuoka University,
3−5−1, Johoku, Naka-ku, Hamamatsu, Shizuoka 432−8561

[*]Graduate School of Materials Science and Technology, Shizuoka University,
3−5−1, Johoku, Naka-ku, Hamamatsu, Shizuoka 432−8561

[**]Development Planning Division, Taiyo Yuden Co., Ltd., 8−1, Sakae-cho, Takasaki, Gunma 370−8522

[***]Institute for Materials Research, Tohoku University, 2−1−1, Katahira, Aoba-ku, Sendai, Miyagi 980−8577

[****]Department of Metallurgy and Ceramics Science, 2−15−1, O-okayama, Meguro-ku, Tokyo 152−8550

Polycrystalline Dy-doped SrTiO₃ thin films deposited by pulsed laser deposition (PLD) on CeO₂-buffered yttria-stabilized zirconia (YSZ) single crystal substrates showed oxygen sensing characteristics at room temperature. The oxygen gas sensing characteristics depended on the amount of Dy-doping, and 1.5 mol% Dy-doping was most effective. The oxygen gas sensing characteristics were closely related to leakage current characteristics of Dy-doped SrTiO₃ thin film deposited on ZnIn₂O₄/YSZ/Si(001) substrates. The suppression of leakage current by Dy-doping suggests that Ti⁴⁺ is substituted by Dy³⁺, and the Dy³⁺ acts as an acceptor. Further doping of Dy³⁺ brought about the increase of the leakage current, and it lowered the oxygen gas sensitivity.

1. Introduction

Oxygen sensors can be classified into two categories. One category is a solid electrolyte type using an yttria-stabilized zirconia (YSZ) and a calcia-stabilized zirconia (CSZ).[1)] Although YSZ and CSZ are the most popular materials, they have a common problem that the operation temperature as the oxygen sensor is limited at around 700–800°C, and it is impossible to use at much higher temperature due to a coexistence of an electron conduction. Another category is a resistive type.[2)] For the category, oxide semiconductors such as ZnO,[3),4)] TiO₂,[5)] V₂O₅–TiO₂,[6)] WO₃,[7)] Gd₂O₃,[8)–10)] and SrTiO₃[11),12)] have been used. The merit of these semiconductor-type oxygen sensors is a wide-range operation temperature from room temperature to around 1000°C. Among these materials, a SrTiO₃ is receiving increased attention because the SrTiO₃ is stable over a large temperature range. Moreover, the SrTiO₃ is expected to be used as an oxygen sensor material in a lean-burn engine system that suppresses a NOₓ generation, and improves an energy efficiency simultaneously.[13)] The SrTiO₃ shows oxygen sensing properties in both p- and n-type semiconductor states. As p-type oxygen sensors, Mg-doped SrTiO₃[13),14)] and Fe-doped SrTiO₃[15),16)] have been reported and as a n-type sensor, SrTiO₃ without dopant[17)] has been reported. In an n-type semiconductor, the resistivity decreases with decreasing an oxygen partial pressure, and in a p-type semiconductor, the resistivity increases with decreasing an oxygen partial pressure. In any cases, the SrTiO₃ thin films can be used as the

oxygen sensors. For an n-type SrTiO₃ thin film, it has been shown that a control of the resistance is important for an oxygen gas sensitivity, and the sample having low resistance does not show the oxygen sensing properties.[17)] This suggests that the control of the carrier concentration is important.

On the other hand, SrTiO₃ thin films have attracted a great attention for use as new capacitor due to high dielectric constant. It is known that the control of an oxygen nonstoichiometry is significantly important for the electrical properties of the films, and if SrTiO₃ thin film contains oxygen vacancies, the leakage current is enhanced according to following equation:

$$O_O^X \rightarrow \frac{1}{2}O_2 + V_O^{\cdot\cdot} + 2e^- \qquad (1)$$

The defect notation is that proposed by Kröger and Vink.[18)] To suppress the leakage current, an acceptor doping of Fe or Cr[19)] and Mn[20)] has been carried out. In this work, the effect of Dy-doping on the electrical and oxygen sensing properties of SrTiO₃ thin film was examined.

Thus far, the effect of Dy-doping on the properties of SrTiO₃ has been reported from the point of diffusion and thermoelectric properties. Yamaji measured a self diffusion coefficient of SrTiO₃ ceramics doped with Dy, and reported that an activation energy of the diffusion increased with the amount of Dy.[21)] He also reported that a grain size of SrTiO₃ ceramics decreased with the amount of Dy due to a segregation of Dy at grain boundaries of SrTiO₃. Muta et al. examined an effect of Sr substitution with a rare earth (Y, La, Sm, Gd and Dy) on thermoelectric properties of SrTiO₃, and they found that a sample doped with Dy (Sr₀.₉Dy₀.₁TiO₃) showed the highest figure of merit.[22)] On the

† Corresponding author: N. Wakiya; E-mail: tnwakiy@ipc.shizuoka.ac.jp

other hand, there are many reports concerning the effect of Dy-doping on the properties of BaTiO₃.[23]–[27] Kim et al. and Kishi et al. reported that the Dy-doping helped a microstructural development with fine grains[23] and enhanced a core-shell structure,[27] respectively. In any cases, the effect of Dy-doping on the oxygen sensing properties is not clarified thus far.

2. Experimental

In this work, all films were prepared by pulsed laser deposition (PLD) using a KrF excimer laser ($\lambda = 248$ nm). At first, 300 nm-thick Dy-doped SrTiO₃ (Dy–ST) thin films were deposited on (In₂O₃–ZnO)(IZO)/YSZ buffered Si(001) substrates. The deposition conditions were shown in **Table 1**. The thicknesses of the IZO oxide bottom electrode layer and YSZ buffer layer were 200 and 50 nm, respectively. After deposition of the Dy–ST layer, Au top electrodes (200 μmϕ) were fabricated by dc sputtering using a metal mask. Electrical properties (current-voltage (*I*–*V*) characteristics, polarization-electric field (*P*–*E*) characteristics, and dielectric constant measurements) were measured. The amount of Dy-doping was 0.4–2.0 mol% of SrTiO₃. In this work, sintered ceramic discs were used as the targets of PLD. To synthesize the targets, reagent grade SrCO₃ and TiO₂ powders with stoichiometric composition were weighted and prescribed amount of DyCl₃ ethanol solution (0.5 M) was added, and mixed with a pestle and a mortar. The powder mixture was calcined at 800°C for 2 h in air. Calcined powders were ground and pressed into pellets, and sintered at 1450°C for 8 h in air.

The deposition conditions of the YSZ, IZO and Dy–ST layers were shown in Table 1. The *I*–*V* and *P*–*E* characteristics were measured using a ferroelectric testing system (Model 6252 Rev.C with HVA–400, Toyo Corp.) and the dielectric constant was measured by an impedance analyzer (4194A, Agilent Technology).

To measure an oxygen sensing property, 300 nm-thick Dy–ST films were deposited on 200 nm-thick CeO₂-buffered YSZ(001) single crystals. The deposition conditions for the films were shown in **Table 2**. The amount of Dy-doping was same as mentioned above. Deposition conditions of CeO₂ were also shown in Table 2. After deposition of the Dy–ST films, Pt surface electrodes were fabricated using a metal mask. Detailed measurement conditions were described in our previous paper.[17] In this work, the resistance of the films was measured at room temperature both in air and in He atmosphere, then the sensitivity was calculated as the difference of resistance (R(in air)–R(in He)). The crystal structure of the films was measured using an X-ray

diffraction (Rint 2200, Rigaku Co.). The composition of the film was examined using an energy dispersive X-ray fluorescent spectroscopy (Minipal + FP Multi, PANalytical).

3. Results and discussion

Figures 1(a) and (b) show XRD patterns of 2 mol% Dy-doped ST thin films deposited on the IZO/YSZ/Si(001) and CeO₂/YSZ(001), respectively. These figures indicate that the Dy-doped ST thin films are polycrystalline. Figure 1(a) also indicates that a coexistence of In₂O₃ is observed. Note that the coexistence was not observed for the IZO/YSZ/Si(001) thin films. Therefore, the coexistence of the In₂O₃ indicates that a partial decomposition of the IZO occurred during the deposition of Dy–ST. The partial decomposition of the IZO is caused by the difference of deposition temperature between the IZO and Dy–ST. As shown in Table 1, the IZO film was deposited at 300°C while Dy–ST film was deposited at 700°C. Resultant phases after the deposition of Dy–ST thin film were unchanged irrespective of the amount of Dy-doping up to 2 mol%. In this work, a further doping of Dy into ST (over 2 mol%) was also tried; however, the further doping caused a lowering of sinterability of the pellets that were used as the target. Therefore, it was impossible to prepare the thin film with further Dy-doping. For the ST thin film without Dy-doping, we measured the composition of the film using an XRF. The analytical composition was Sr/Ti = 1.26. This means that the film has a Sr-rich composition. However, as shown in Fig. 1, the XRD pattern indicates that a single phase SrTiO₃ film was prepared irrespective of the Sr-rich composition. This means that an excess Sr is incorporated into the SrTiO₃ lattice. Such wide range of solid solution is frequently observed in the case of thin film.[28]

Figure 2 shows the change of lattice parameter of Dy–ST thin film with the amount of Dy-doping. This figure depicts that the lattice parameter increases with the amount of Dy-doping. The ionic radius of Sr²⁺ (12-fold coordination), Ti⁴⁺ (6-fold coordination), and Dy³⁺ (6-fold coordination) is 0.144, 0.0605 and 0.0912 nm, respectively.[29] On the other hand, that of Dy³⁺ in 12-fold coordination has not been reported. For Dy³⁺, ionic radii have been reported for 6, 7, 8 and 9-fold coordinations. In this work, the ionic radius of Dy³⁺ in 12-fold coordination was estimated from the extrapolation as shown in **Fig. 3**. As the result, the ionic radius was estimated as 0.1255 nm. Note that both ionic radii of Dy³⁺ in 6- and 12-fold coordinations are larger than that of Ti⁴⁺

Table 1. Deposition Conditions of Dy–ST/IZO/YSZ Thin Film on Si(001) Substrate

	Deposition temperature (°C)	Deposition pressure (Torr)	Thickness (nm)
YSZ	800	5.5×10^{-6}	50
ZnIn₂O₄ (IZO)	300	5.5×10^{-6}	200
Dy-dopedSrTiO₃ (Dy–ST)	700	1.0×10^{-2}	300

Table 2. Deposition Conditions of Dy–ST/CeO₂ Thin Film on YSZ(001) Substrate

	Deposition temperature (°C)	Deposition pressure (Torr)	Thickness (nm)
CeO₂	800	5.5×10^{-6}	200
Dy-dopedSrTiO₃ (Dy–ST)	700	1.0×10^{-2}	300
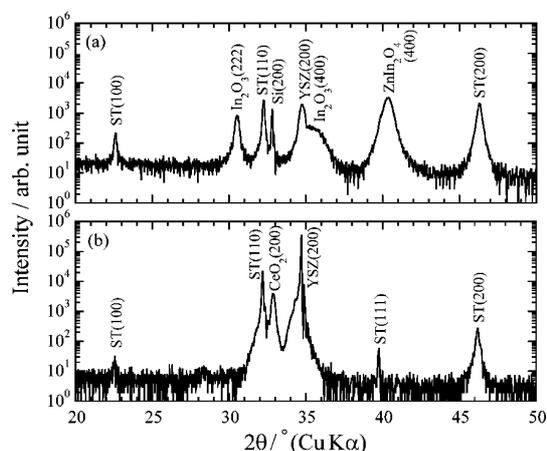
Fig. 1. XRD pattern of (a) Dy–ST/IZO/YSZ/Si(100) and (b) Dy–ST/CeO₂/YSZ(100).
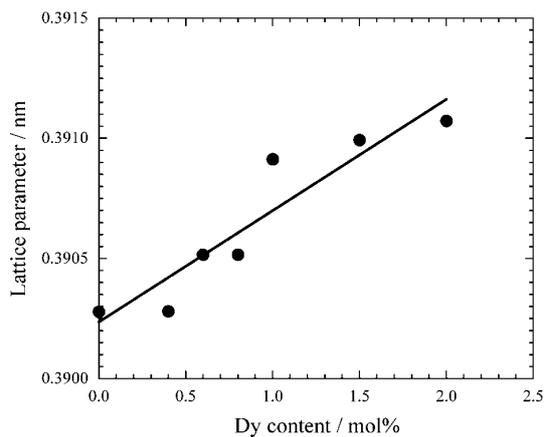
Fig. 2. Change of lattice parameter of Dy–ST thin film with the amount of Dy -doping.
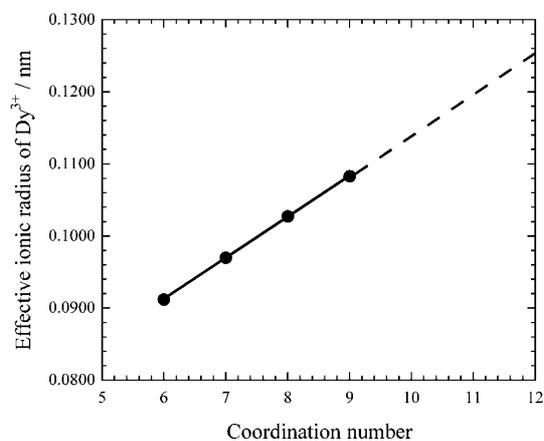
Fig. 3. Estimation of ionic radius of Dy^{3+} in 12-fold coordination by extrapolation of ionic radii reported by Shannon.[29]

Fig. 4. Change of current-voltage characteristics with the amount of Dy-doping. (a), (b), (c) and (d) denote that the amount of Dy-doping is 0, 1.0, 1.5 and 2.0 mol%, respectively. Inset (1) shows change of current-voltage characteristics of Mn-doped SrTiO₃ thin film prepared by RF sputtering reported by Morito et al..[20] Inset (2) shows change of resistivity for Dy-doped BaTiO₃ ceramics reported by Lee et al..[24]

(6-fold coordination), and are smaller than that of Sr^{2+} (12-fold coordination). The fact that the lattice parameter of SrTiO₃ increases with Dy-doping suggests that the Ti^{4+} predominantly substituted by Dy^{3+}. To consider the possibility of B-site substitution, electrical properties of the film was also examined.

After fabrication of Au top electrodes on the surface of Dy–ST/IZO/YSZ/Si(001) thin film, the change of current-voltage (I–V) characteristics with the amount of Dy was measured between the Au top and IZO bottom electrodes, and the I–V curves were shown in **Fig. 4**. The ST thin film without Dy-doping showed a significant amount of leakage current (4.4×10^1 A/cm² at 100 kV/cm) as shown in Fig. 4(a). The doping of 1.0 and 1.5 mol% Dy brings about the decrease of leakage current (5.0×10^0 A/cm² and 3.5×10^{-1} A/cm², respectively at 100 kV/cm) as shown in Figs. 4(b) and(c). On the other hand, further Dy-doping brings about the increase of leakage current. Figure 4(d) indicates that the doping of 2 mol% Dy brings about a higher leakage current (3.0×10^0 A/cm² at 100 kV/cm). To consider the effect of Dy-doping into SrTiO₃ on the leakage current, previously reported data are also shown as the insets of Fig. 4 for comparison. The inset (1) shows the change of I–V curves with the amount of Mn-doping into SrTiO₃ thin film prepared by RF sputtering.[20] This figure indicates that small amount of Mn-doping (0.2 mol%) brings about the decrease of leakage current and further doping

(5 mol%) brings about the increase of leakage current. This behavior is very close to our results shown above. Note that Mn^{3+} has been believed to be incorporated into the Ti^{4+} site to act as an acceptor.[20] The fact that the Dy-doping into SrTiO₃ showed a similar tendency with the Mn-doping into SrTiO₃ suggests that the Dy^{3+} is incorporated into the Ti^{4+} site. This consideration agrees well with the discussion mentioned to explain the result of Fig. 2. On the other hand, the inset (2) of Fig. 4 shows the change of resistivity of BaTiO₃ ceramics with the amount of Dy-doping. This figure indicates that a small amount of Dy-doping up to 0.2–0.3 mol% drastically decreases the resistivity of BaTiO₃, and further Dy-doping increases the resistivity. This dependency is the opposite of our results. For the Dy-doped BaTiO₃, Ba^{2+} is substituted with Dy^{3+} to act as a donor.[24] Therefore, our consideration that the Ti^{4+} is substituted with Dy^{3+} for Dy-doped SrTiO₃ thin film is plausible.

By the comparison of our data (Dy-doped ST) with the inset (1) (Mn-doped ST), the magnitude of the leakage current density of our data is much larger than that of the Mn-doped ST. As the reason of the difference, two possibilities can be considered. One possibility is due to the composition that our film has Sr-rich composition mentioned above. If the excess Sr is incorporated into the interstitial site, the leakage current increases due to the generation of electron as

$$Sr \rightarrow Sr_i^{\bullet\bullet} + 2e^- \qquad (2)$$

Another possibility is due to the difference of the thin film deposition method. In general, the films prepared by PLD include considerable amount of oxygen vacancies, and the oxygen vacancies bring about the electron according to the Eq. (1) shown in the introduction session. In any possibilities, our ST thin film includes considerable amount of electrons that increase the leakage current. The decrease of the leakage current by Dy-doping up to 1.5 mol% as shown in Fig. 4 can be interpreted that the Dy^{3+} acts as an acceptor and hole is recombined with electron;

$$2SrO + Dy_2O_3 + \frac{1}{2}O_2 \rightarrow 2Sr_{Sr}^X + 2Dy_{Ti}' + 6O_O^X + 2h^{\bullet} \quad (3)$$
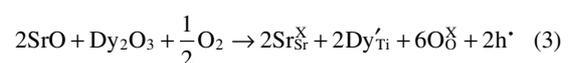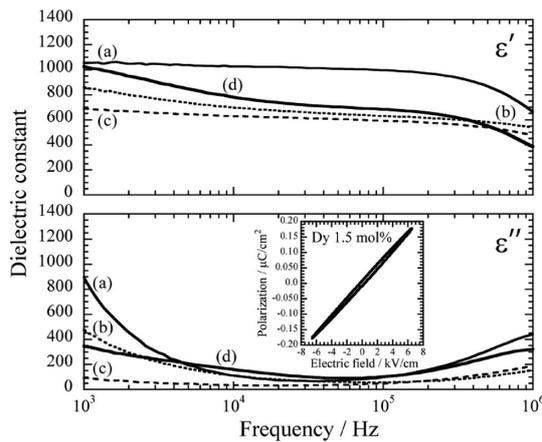
Fig. 5. Frequency dependence of dielectric constant of (a) ST, (b) 1.0 mol% Dy-doped ST, (c) 1.5 mol% Dy-doped ST and (d) 2.0. mol% Dy-doped ST. Upper and lower spectrum is ε' and ε'', respectively. *P–E* curve of 1.5 mol% Dy-doped ST is shown in the inset.

$$e' + h^\bullet \rightarrow null \tag{4}$$

The reason why leakage current was increased by 2.0 mol% Dy-doping can be explained by following three possibilities.

The first is the generation of a hole according to Eq. (3), and the second is generation of an electron according to Eq. (5).

$$Dy_2O_3 + TiO_2 \rightarrow 2Dy^\bullet_{Sr} + 2Ti^X_{Ti} + 6O^X_O + \frac{1}{2}O_2 + 2e' \tag{5}$$
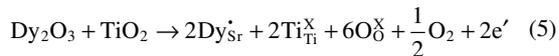
The third is due to the change of microstructure by the Dy-doping. To determine which possibility is most plausible, additional methods such as Seebeck coefficient measurements and microstructure observation is needed.

Figure 5 shows the change of a frequency dependency of dielectric constant of the Dy-doped ST thin film. This figure indicates that 1.5 mol% Dy-doped ST thin film has small frequency dependencies in ε' and low ε''. The *P–E* curve of 1.5 mol% Dy-doped ST was also shown as the inset of Fig. 5. The facts that 1.5 mol% Dy-doped ST thin film has low ε'' and paraelectric characteristics agree that the film has the lowest leakage current as shown in Fig. 4. The fact that the 1.5 mol% Dy-doped ST thin film showed paraelectric characteristics means that a local ferroelectricity[30] is not brought about by the Dy-doping.

The effect of the Dy-doping on the O_2 gas sensor characteristics was measured after fabrication of Pt surface electrodes on a Dy–ST/CeO$_2$/YSZ(100) thin film. In this work, the resistance of the film surface was measured both in air and in He atmosphere. **Figure 6**(a) shows the change of the resistance with the amount of Dy-doping. This figure indicates that no change in surface resistance was observed for the ST thin film without Dy-doping, and the change was observed by the Dy-doping. In this work, the sensitivity for an oxygen gas was defined by a difference of resistance:

$$(\text{Sensitivity}) = R \text{ (in air)} - R \text{ (in He)} \tag{6}$$

The change of the sensitivity with the Dy content was shown in Fig. 6 (b). This figure clearly shows that a maximum sensitivity was observed at 1.5 mol% of Dy-doping. By comparison of Figs. 4, 5 and 6, it can be mentioned that the sensitivity for an oxygen gas is closely related to the leakage current, and to improve the oxygen sensitivity, it is important to suppress the leakage current. Hara et al.[17] examined the effect of Nb-doping into a SrTiO$_3$ thin
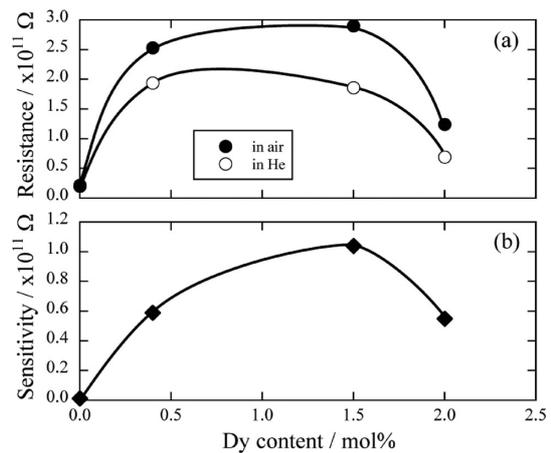
Fig. 6. Change of (a) resistance and (b) sensitivity of Dy-doped ST thin film with the amount of Dy-doping.

film on the oxygen sensitivity, and they found that the sensitivity decreases by a carrier doping. The result of the Dy-doping agrees well with the report. Therefore, to improve the oxygen sensitivity, we believe co-doping of other elements such as Mn^{3+} and Fe^{3+} with Dy^{3+} is effective.

4. Conclusions

PLD prepared Dy-doped SrTiO$_3$ polycrystalline thin films were investigated for their potential application as an oxygen gas sensor operated at room temperature. The experimental results revealed that the oxygen gas sensitivity was close to the leakage current of the film and the maximum oxygen sensitivity was obtained at 1.5 mol% of Dy. At the Dy content, the leakage current showed minimum value. The suppression of the leakage current by Dy-doping suggests that Ti^{4+} is substituted by Dy^{3+}, and the Dy^{3+} acts as an acceptor. Further doping of Dy^{3+} brought about the increase of leakage current and lowered the oxygen gas sensitivity.

References

1) D. T. Dimitrov, C. D. Dushkin, N. L. Petrova, R. V. Todorovska, D. S. Todrovsky, S. Y. Anastasova and D. H. Oliver, *Sensors and Actuators A*, **137**, 86–95 (2007).
2) S. Pitcher, J. A. Thiele, H. Ren and J. F. Vetelino, *Sensors and Actuators B*, **93**, 454–462 (2003).
3) J. J. Osborne, G. T. Roberts, A. R. Chambers and S. B. Gabriel, *Sensors and Actuators B*, **63**, 55–62 (2000).
4) N. Golego, S. A. Studenikin and M. Cocivera, *J. Electrochem. Soc.*, **147**[4], 1592–1594 (2000).
5) L. Castaneda, *Mater. Sci. Eng. B*, **139**, 149–154 (2007).
6) S. Zhuiykov, W. Wlodarski and Y. Li, *Sensors and Actuators B*, **77**, 484–490 (2001).
7) R. Boulmani, M. Bendahan, C. Lambert-Mauriat, M. Gillet and K. Aguir, *Sensors and Actuators B*, **125**, 622–627 (2007).
8) M. Ogita, K. Higo, Y. Nakanishi and Y. Hatanaka, *Appl. Surf. Sci.*, **175–176**, 721–725 (2001).
9) C. I. Baban, Y. Toyoda and M. Ogita, *Jpn. J. Appl. Phys.*, **43**[10], 7213–7216 (2004).
10) C. Baban, Y. Toyoda and M. Ogita, *Thin Solid Films*, **484**, 169–373 (2005).
11) Y. Hu, O. K. Tan, W. Cao and W. Zhu, *Ceram. Int.*, **30**, 1819–1822 (2004).
12) Y. Hu, O. K. Tan, J. S. Pan. H. Huang and W. Cao, *Sensors and Actuators B*, **108**, 244–249 (2005).
13) T. Ding and W. Jia, *Sensors and Actuators B*, **82**, 284–286

(2002).

14) H. Zheng and O. T. Sorensen, *Sensors and Actuators B*, **65**, 299–301 (2000).

15) M. M. Kumar and M. L. Post, *J. Appl. Phys.*, **97**, 114916-1–114916-8 (2005).

16) S. J. Litzelman, A. Rothschild and H. L. Tuller, *Sensors and Actuators B*, **108**, 231–237 (2005).

17) T. Hara, T. Ishiguro, N. Wakiya and K. Shinozaki, *Jpn. J. Appl. Phys.*, **47**[9], 7486–7489 (2008).

18) F. A. Kröger and H. J. Vink, *Solid State Physics* (Academic Press, New York, 1956).

19) S. H. Paek, E. S. Lee, S. H. Kim, J. Y. Seong, J. P. Mah, C. S. Park, J. S. Choi and J. H. Jung, *J. Mater. Sci.*, **33**, 1239–1242 (1998).

20) K. Morito, T. Suzuki and M. Fujimoto, *Jpn. J. Appl. Phys.*, **40**[9], 5493–5496 (2001).

21) A. Yamaji, *Denkitsuushin Kennkyuujyo Kenkyuu Jitsuyouka Houkoku,* **25**[7], 1197–1205 (1976)[in Japanese].

22) H. Muta, K. Kurosaki and S. Yamanaka, *J. Alloy Compd.*, **350**[1–2], 292–295 (2003).

23) H. T. Kim and Y. H. Han, *Ceram. Int.*, **30**, 1719–1723 (2004).

24) E. J. Lee, J. Jeong and Y. H. Han, *Jpn. J. Appl. Phys.*, **43**[12], 8126–8129 (2004).

25) E. J. Lee, J. Jeong and Y. H. Han, *Jpn. J. Appl. Phys.*, **45**[2], 822–825 (2006).

26) H. Miao, M. Dong, G. Tan and Y. Pu, *J. Electroceram.*, **16**, 297–300 (2006).

27) H. Kishi, N. Kohzu, J. Sugino, H. Ohsato, Y. Iguchi and T. Okuda, *J. Euro. Ceram. Soc.*, **19**, 1043–1046 (1999).

28) D. Nagano, H. Funakubo, K. Shinozaki and N. Mizutani, *Appl. Phys. Lett.*, **72**[16], 2017–2019 (1998).

29) R. D. Shannon, *Acta Cryst. A*, **32**, 751–767 (1976).

30) O. Tikhomirov, H. Jiang and J. Levy, *Appl. Phys. Lett.*, **77**, 2048–2050 (2000).